Synthesis and Structure of New Layered Oxides, $M^{II}La_2Ti_3O_{10}$ (M = Co, Cu, and Zn)

Ki-An Hyeon and Song-Ho Byeon*

Department of Chemistry, College of Natural Sciences, Kyung Hee University, Kyung Ki 449-701, Korea

Received August 19, 1998. Revised Manuscript Received October 15, 1998

New layered perovskite compounds, $M^{II}[La_2Ti_3O_{10}]$ (M = Co, Cu, and Zn) were synthesized by the ion-exchange reaction of the parent $Na_2La_2Ti_3O_{10}$ in molten salts. The crystal structure of the as-synthesized phases was determined by the Rietveld refinement for the powder X-ray diffraction patterns. The unit cells are tetragonal with a = 3.8128(1), 3.8248(2), and 3.8127(1) Å and c = 27.568(1), 26.329(1), and 27.5129(9) Å with an $I4/mmm$ (Z = 2) space group for the Co, Cu, and Zn phases, respectively. The transition-metal atoms occupy strongly flattened tetrahedral sites with 50% probability between the perovskite slabs. These oxides represent the first example of layered perovskite whose interlayer spaces are occupied by small transition-metal cations. Particularly for the Cu oxide, remarkable shortening of the c-axis was observed upon heating up to 700 °C under an Ar atmosphere. Such a contraction is likely to result from the flattening of the CuO_4 unit toward a quasi-square planar coordination.

Introduction

Recently, there was considerable interest in two types of layered oxides derived from the ABO_3 perovskite structure. One is the Ruddlesden−Popper series[1,2] of the general formula $A'_2[A_{n-1}B_nO_{3n+1}]$ where $[A_{n-1}B_nO_{3n+1}]$ perovskite-like slabs are interleaved by A′ cation layers. The large A cations occupy 12-coordinate sites as found in the perovskite lattice. Layered oxides of the general formula $A'[A_{n-1}B_nO_{3n+1}]$ (A′ = alkali metal)[3] are similar to the Ruddlesden−Popper series but different in the interlayer cation density. The thickness of each perovskite slab is given by the value n that determines the number of BO_6 octahedra corner-shared perpendicular to the layers. Both the series of solids easily exchange interlayer alkali-metal cations in molten salt or under acidic conditions.[2,4−6]

Because of the existence of two different series of layered oxides with the same perovskite slab, a system $A'_{2-x}La_2Ti_{3-x}Nb_xO_{10}$ ($0 \le x \le 1$, A = K and Rb) was investigated.[7] This system corresponds to the solid solution between $A'_2[La_2Ti_3O_{10}]$ and $A'[La_2Ti_2NbO_{10}]$ which are n = 3 members of each series. This solid solution having a variable interlayer cation density could be thus regarded as bridging the two series of layered perovskites. More importantly, a decrease of cation density must be accompanied by a formation of vacancies in A′ cation layers. The existence of interlayer vacancies exposes the structure to further chemistry. For instance, $Rb_2[LaNb_2O_7]$ (n = 2 member of the Ruddlesden−Popper series) can be prepared by Rb vapor intercalation into 50% vacant interlayer sites of $Rb[LaNb_2O_7]$.[8] In this case, an increase of interlayer charge is compensated for by the reduction of a $[LaNb_2O_7]$ layer charge giving rise to the 4+/5+ mixed valency of Nb. If the layer charge is kept constant, therefore, it was expected that the exchange between one divalent cation and two monovalent ones would be possible in the same host oxides. The exchange of multivalent cations for monovalent ones has been widely studied in clay minerals.[9−11] The interlayer cations, which are ion-exchangeable, are normally Na^+ and Ca^{2+} but a transition-metal ion can also be exchanged. On the contrary, there have been few studies on such an exchange behavior in a perovskite-related compound. During our work, one example was reported; the exchange between Ca^{2+} and Na^+ of a similar size was carried out with $NaLaTiO_4$.[12]

In this work, we explored the exchange of the interlayer Na^+ ion in $Na_2[La_2Ti_3O_{10}]$ (n = 3 member of the Ruddlesden−Popper series) by much smaller M^{2+} ones (M = transition metals) in molten salts. Except $ZnCl_2$, however, most of the salts containing divalent transition-metal cations have too high of a melting point for the ion-exchange reaction. Fortunately, the exchange

* To whom correspondence should be addressed.

(1) Ruddlesden, S. N.; Popper, P. *Acta Crystallogr.* **1957**, *10*, 538.
(2) Gopalakrishnan, J.; Bhat, V. *Inorg. Chem.* **1987**, *26*, 4299.
(3) Dion, M.; Ganne, M.; Tournoux, M. *Mater. Res. Bull.* **1981**, *16*, 1429.
(4) Jacobson, A. J.; Lewandowski, J. T.; Johnson, J. W. *J. Less-Common Met.* **1986**, *116*, 137.
(5) Gopalakrishnan, J.; Bhat, V.; Raveau, B. *Mater. Res. Bull.* **1987**, *22*, 413.
(6) Subramanian, M. A.; Gopalakrishnan, J.; Sleight, A. W. *Mater. Res. Bull.* **1988**, *23*, 837.
(7) Uma, S.; Raju, A. R.; Gopalakrishnan, J. *J. Mater. Chem.* **1993**, *3*, 709.
(8) Armstrong, A. R.; Anderson, P. A. *Inorg. Chem.* **1994**, *33*, 4366.
(9) Grim, R. E. *Clay Mineralogy*, 2nd ed.; McGraw-Hill: New York, 1968.
(10) Barrer, R. M. *Hydrothermal Chemistry of Zeolites*; Academic Press: New York, 1982.
(11) Kalogirou, O. *J. Solid State Chem.* **1993**, *102*, 318.
(12) McIntyre, R. A.; Falster, A. U.; Li, S.; Simmons, W. B., Jr.; O'Connor, C. J.; Wiley, J. B. *J. Am. Chem. Soc.* **1998**, *120*, 217.

10.1021/cm980581f CCC: $18.00
Published on Web 12/29/1998

reaction between Na^+ and some M^{2+} ions was successfully carried out with an eutectic-like salt which is obtained by mixing KCl and MCl_2 with an appropriate ratio. Here, we describe in detail the synthesis and structure of new layered perovskite compounds of the general formula $M^{II}[La_2Ti_3O_{10}]$ (M = Co, Cu, and Zn). As far as we know, these oxides represent the first example of layered perovskite whose interlayer spaces are occupied by small transition-metal cations.

Experimental Section

Synthesis. Parent-layered perovskite, $Na_2La_2Ti_3O_{10}$, was prepared by heating an appropriate mixture of Na_2CO_3, La_2O_3, and TiO_2 in air at 1050 °C for 2 days with two intermittent grindings. An excess (~20 mol %) of Na_2CO_3 was added to compensate for the loss of the volatile sodium component. After the reaction, the product was washed with distilled water and dried at 120 °C.

Because of a high melting temperature of $CoCl_2$ (m.p. = 735 °C) and $CuCl_2$ (m.p. = 620 °C), a mixture with potassium chloride was required for the exchange reaction of Co^{2+} and Cu^{2+} for Na^+. Thus, $CoLa_2Ti_3O_{10}$ could be prepared by treating 1 g of $Na_2La_2Ti_3O_{10}$ with 30 g of molten mixture of molar composition 50% $CoCl_2$ and 50% KCl at 420 °C for 2 weeks. Similarly, $CuLa_2Ti_3O_{10}$ could be prepared by treating 1 g of $Na_2La_2Ti_3O_{10}$ with 30 g of molten mixture of molar composition 60% $CuCl_2$ and 40% KCl at 350 °C for 10 days. $ZnLa_2Ti_3O_{10}$ was easily prepared without addition of KCl by heating 1 g of $Na_2La_2Ti_3O_{10}$ with 10 g of molten $ZnCl_2$ (m.p. = 283 °C) at 300 °C for 2 weeks. All the mixtures were replaced once in between. To avoid a formation of corresponding MO oxides on heating MCl_2 in air, a Pyrex flask containing reactants was filled with Ar gas during all of the reaction. After the exchange reaction of Co^{2+} and Cu^{2+} for Na^+ took place, the oxide turned from white to bright purple and bright brown, respectively. The final products were washed with hot water.

A formation of $FeLa_2Ti_3O_{10}$ was also examined by using the mixture of molar composition 50% $FeCl_2$ and 50% KCl at 420 °C according to the same procedure. In addition, a synthesis of $NiLa_2Ti_3O_{10}$ was tried with the mixture of 70% $NiCl_2$ and 30% KCl at 500 °C. However, it was difficult to avoid the formation of Fe_2O_3 and NiO as major impurity phases.

Characterizations. The absence of the sodium component in the ion-exchanged products was confirmed by the inductively coupled plasma (ICP) analysis. No potassium component was detected and a possibility of an exchange reaction between Na^+ and K^+ ions could be accordingly ruled out.

Elemental analysis using the energy-dispersive X-ray emission (EDX) and ICP techniques gave a stoichiometric composition for the Co and Cu compounds (Co or Cu:La:Ti = 1:2:3) within experimental errors. Because of the similar emission range of Zn and La on EDX analysis, a stoichiometric composition of the Zn analogue was confirmed by ICP only.

The formation of a single phase was confirmed by powder X-ray diffraction (XRD). The patterns for structure refinement were recorded on a rotating anode installed diffractometer with an X-ray source of 40 kV, 300 mA. The Cu Kα radiation used was monochromated by a curved-crystal graphite. The data were collected with a step-scan procedure in the range 2θ = 10−110° with a step width of 0.02° and a step time of 1 s. The refinement of reflection positions and intensities were carried out using the Rietveld analysis program RIETAN.[13]

Results and Discussion

Structure Refinement. The XRD patterns of $M^{II}La_2Ti_3O_{10}$ (M = Co, Cu, and Zn) were comparable with that of the parent $Na_2La_2Ti_3O_{10}$ (a = 3.834 Å and c = 28.65 Å).[15] The presence of strong low-angle reflections and the similarity of the patterns to that of the parent oxide suggested that the layer-type structure is retained after the exchange reaction. We could accordingly index all of the reflections of $M^{II}La_2Ti_3O_{10}$ on a tetragonal symmetry with the cell parameters $a \sim 3.8$ Å and $c \sim 27$ Å. A contraction along the c-axis with respect to the parent $Na_2La_2Ti_3O_{10}$ was consistent with the exchange of Na^+ by smaller Co^{2+}, Cu^{2+}, and Zn^{2+}. Observed c-axis doubling (~27 Å) indicated that a relative displacement of adjacent perovskite slabs toward staggered conformation is also retained. The reflection condition found for these phases was $h + k + l = 2n$ for hkl reflections, leading to the I-type unit cell of eight possible space groups. In the first stage, therefore, the crystal structure of $M^{II}[La_2Ti_3O_{10}]$ was refined using initial atomic positions (space group $I4/mmm$) of $Na_2Ln_2Ti_3O_{10}$.[14,15] Because of the fact that the exchange reaction in our work must give rise to 50% vacancies in the interlayer spaces of the parent oxide, the occupancy factor of M for the position 4e was kept at 0.5 during refinement. A similar structure model was proposed for β-$Na[Ca_2Nb_3O_{10}]$[3,16] In this structure, divalent metal ions would thus be statistically distributed at one-half of the sodium positions in $Na_2La_2Ti_3O_{10}$. Such a site may be unusually large for the stabilization of small transition-metal cations because it is coordinated by nine oxygen ions. Indeed, this refinement gave poor reliability factors and large or negative isotropic temperature factors. Since the c-axis doubling is not induced when A is large, the structure of $A[Ca_2Nb_3O_{10}]$ where A = Cs, Rb was not considered as a possible structure for $M^{II}[La_2Ti_3O_{10}]$. A structure model suggested for α-$Na[Ca_2Nb_3O_{10}]$[3] was then adopted for better refinement. The interlayer space between adjacent perovskite slabs is composed of tetrahedral sites coordinated by four oxygen ions in such a structure, one-half of which are occupied by divalent cations with an ordered manner. A number of possible tetragonal space groups consistent with this model of doubled a- (~7.7 Å) and/or c- (~52 Å) axes were tested, with $I4_1/acd$ giving the best reliability factors. However, none of these models gave a good fit with reasonable positional and isotropic thermal parameters. When the position of M is shifted to 4d (0.0, 0.5, 0.25) rather than 4e (0.0, 0.0, z), the refinement converged rapidly in the space group $I4/mmm$ to agreeable profile fit parameters. Such a position is generally adopted for the interlayer alkali-metal cation in $ALaNb_2O_7$ (A = Li and Na).[17,18] This structural model is different from that of α-$Na[Ca_2Nb_3O_{10}]$ in the fact that the interlayer cations are statistically distributed at one-half of possible tetrahedral sites. Corrections for a (00l) preferred orientation were made for all phases in the final stage of the refinement. Some crystallographic data and the final reliability factors are given in Table 1. The observed, calculated, and difference profiles for all

(13) Izumi, F.; Murata, H.; Watanabe, N. *J. Appl. Crystallogr.* **1987**, *20*, 411.

(14) Richard, M.; Brohan, L.; Tournoux, M. *J. Solid State Chem.* **1994**, *112*, 345.

(15) Toda, K.; Kameo, Y.; Fujimoto, M.; Sato, M. *J. Ceram. Soc. Jpn.* **1994**, *102*, 737.

(16) Dion, M.; Ganne, M.; Tournoux, M. *Rev. Chim. Miner.* **1984**, *21*, 92.

(17) Sato, M.; Abo, J.; Jin, T. *Solid State Ionics* **1992**, *57*, 285.

(18) Sato, M.; Abo, J.; Jin, T.; Ohta, M. *J. Alloys Comp.* **1993**, *192*, 81.

Table 1. Crystallographic Data of $MLa_2Ti_3O_{10}$ where M = Co, Cu, and Zn

	$CoLa_2Ti_3O_{10}$	$CuLa_2Ti_3O_{10}$	$ZnLa_2Ti_3O_{10}$
space group	*I*4/*mmm* (no. 139)	*I*4/*mmm* (no. 139)	*I*4/*mmm* (no. 139)
a (Å)	3.8128(1)	3.8248(2)	3.8127(1)
c (Å)	27.568(1)	26.329(1)	27.5129(9)
Z	2	2	2
V (Å^3)	402.6	385.0	399.9
ρ (g/cm^3)	5.31	5.56	5.37
Bragg (R_I, %)	4.23	6.66	3.15
weighted profile (R_{WP}, %)	13.99	11.51	11.39
profile (R_P, %)	9.69	8.69	8.54
expected (R_E, %)	5.16	4.15	4.94

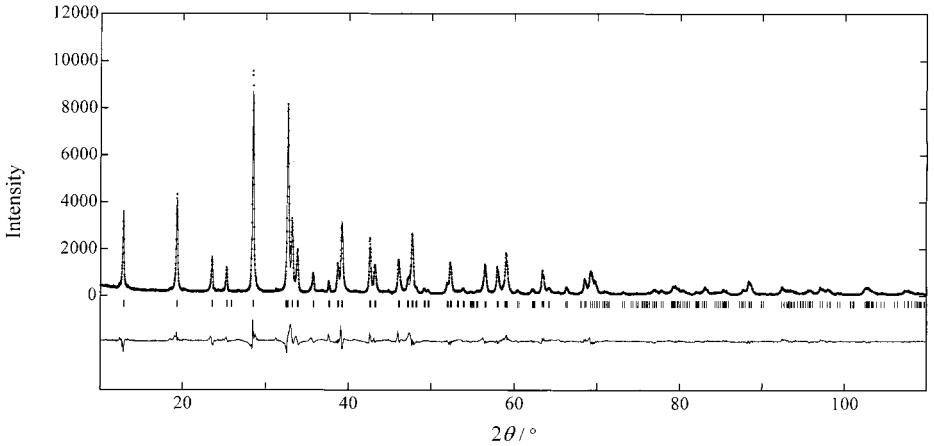

Figure 1. Calculated (solid line), experimental (dotted line), and difference (solid lines on the bottom) X-ray powder diffraction pattern of the as-prepared $CoLa_2Ti_3O_{10}$.

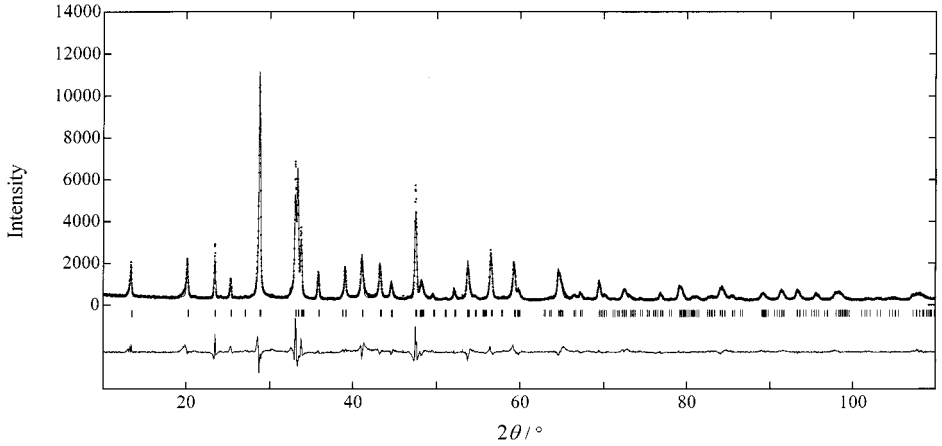

Figure 2. Calculated (solid line), experimental (dotted line), and difference (solid lines on the bottom) X-ray powder diffraction pattern of the as-prepared $CuLa_2Ti_3O_{10}$.

phases are plotted in Figures 1−3. The refined atomic coordinates and isotropic temperature factors are listed in Table 2.

Description of the Structure. Selected bond lengths and bond angles for $M^{II}[La_2Ti_3O_{10}]$ (M = Co, Cu, and Zn) are shown in Table 3. The ideal structure illustrated in Figure 4 is characterized as a two-dimensional framework of the $[La_2Ti_3O_{10}]$ layer perpendicular to the *c*-axis. The triple-perovskite layers consisting of corner-shared TiO_6 octahedra are separated by the transition-metal layers, the adjacent blocks having a staggered conformation of each other. A strongly distorted coordination environment for Ti(2) is revealed, involving a displacement from the center of its octahedron toward the transition-metal layers to give one short Ti(2)-O(3), one long Ti(2)-O(1), and four normal length Ti(2)-O(4) bonds. In contrast to $Ti(2)O_6$ octahedra, a similar bond length of Ti(1)-O(1) and Ti(1)-O(2) gives slightly distorted central $Ti(1)O_6$ octahedra. Such bond characters were also true for the parent $Na_2La_2Ti_3O_{10}$.[15] The O(4)-Ti(2)-O(4) angles are similar for the Co, Cu, and Zn phases, suggesting that a distortion of the $Ti(2)O_6$ octahedron is essentially independent of the nature of the interlayer space.

Figure 5 shows the arrangement of transition-metal atoms in the interlayer spaces. They are surrounded by four O(3) oxygens, forming MO_4 tetrahedra. The next nearest neighboring oxygens, O(4), are at 3.049, 2.74, and 3.062 Å for the Co, Cu, and Zn oxides, respectively. All of these tetrahedral sites are occupied by transition-metal atoms with 50% probability. When the unit cell parameters are concerned, the Cu oxide has the shortest *c*-axis with the longest *a*-axis. This change is contrary to what might be expected from purely size consider-

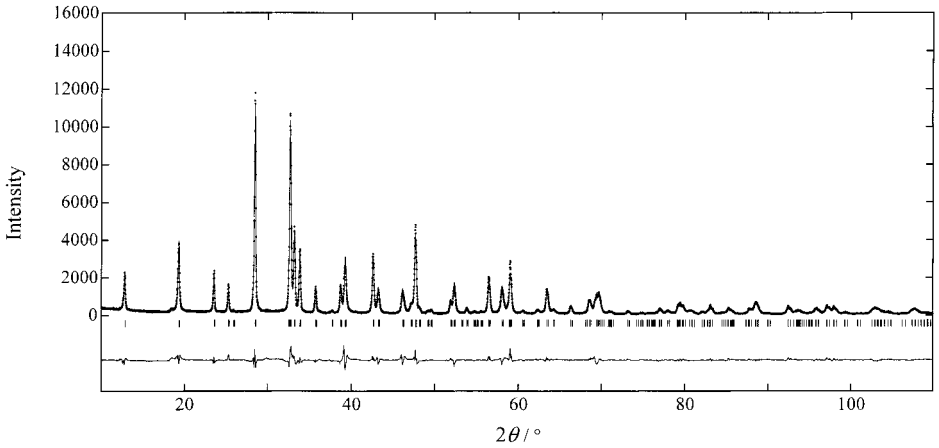

Figure 3. Calculated (solid line), experimental (dotted line), and difference (solid lines on the bottom), X-ray powder diffraction pattern of the as-prepared $ZnLa_2Ti_3O_{10}$.

Table 2. Atomic Positions and Isotropic Temperature Factors of $MLa_2Ti_3O_{10}$ (M = Co, Cu, and Zn)

compound	atom	*g*	*x*	*y*	*z*	*B* (Å^2)
$CoLa_2Ti_3O_{10}$	La	1.0	0.0	0.0	0.4209(1)	0.97(5)
	Co	0.5	0.0	0.5	0.25	1.0(2)
	Ti(1)	1.0	0.0	0.0	0.0	0.6(1)
	Ti(2)	1.0	0.0	0.0	0.1547(2)	0.42(9)
	O(1)	1.0	0.0	0.0	0.0756(6)	2.1(5)
	O(2)	1.0	0.0	0.5	0.0	2.8(6)
	O(3)	1.0	0.0	0.0	0.2203(3)	0.7(3)
	O(4)	1.0	0.0	0.5	0.1406(3)	1.4(3)
$CuLa_2Ti_3O_{10}$	La	1.0	0.0	0.0	0.4175(1)	0.80(7)
	Cu	0.5	0.0	0.5	0.25	1.6(2)
	Ti(1)	1.0	0.0	0.0	0.0	0.7(1)
	Ti(2)	1.0	0.0	0.0	0.1613(2)	0.4(1)
	O(1)	1.0	0.0	0.0	0.0732(6)	0.8(4)
	O(2)	1.0	0.0	0.5	0.0	2.1(8)
	O(3)	1.0	0.0	0.0	0.2269(4)	0.9(9)
	O(4)	1.0	0.0	0.5	0.1458(4)	1.5(3)
$ZnLa_2Ti_3O_{10}$	La	1.0	0.0	0.0	0.4210(1)	0.73(4)
	Zn	0.5	0.0	0.5	0.25	1.2(1)
	Ti(1)	1.0	0.0	0.0	0.0	0.8(2)
	Ti(2)	1.0	0.0	0.0	0.1543(1)	0.6(1)
	O(1)	1.0	0.0	0.0	0.0714(4)	1.3(3)
	O(2)	1.0	0.0	0.5	0.0	2.6(6)
	O(3)	1.0	0.0	0.0	0.2206(3)	0.9(3)
	O(4)	1.0	0.0	0.5	0.1404(2)	0.9(2)

Table 3. Selected Bond Lengths (Å) and Bond Angles (deg) in $MLa_2Ti_3O_{10}$ (M = Co, Cu, and Zn)

	$CoLa_2Ti_3O_{10}$	$CuLa_2Ti_3O_{10}$	$ZnLa_2Ti_3O_{10}$
	Bond Lengths		
M-O(3) (×4)	2.075(4)	2.007(4)	2.071(4)
M-O(4) (×2)	3.049(9)	2.74(1)	3.062(8)
Ti(1)-O(1) (×2)	2.11(2)	1.93(2)	1.96(1)
Ti(1)-O(2) (×4)	1.906(1)	1.912(1)	1.906(1)
Ti(2)-O(1) (×1)	2.15(2)	2.32(2)	2.28(1)
Ti(2)-O(3) (×1)	1.81(1)	1.73(1)	1.823(9)
Ti(2)-O(4) (×4)	1.951(2)	1.956(2)	1.944(1)
La-O(1) (×4)	2.697(1)	2.716(1)	2.704(1)
La-O(2) (×4)	2.900(1)	2.893(2)	2.891(1)
	Bond Angles		
O(3)-M-O(3)	133.5(5)	144.7(4)	134.0(2)
	99.0(1)	95.3(1)	98.8(1)
O(4)-Ti(2)-O(4)	157.1(5)	155.9(4)	157.3(3)
	87.7(1)	87.5(1)	87.8(1)

ations because of a similar radius[19] of Co^{2+} (r = 0.58 Å), Cu^{2+}(r = 0.57 Å), and Zn^{2+}(r = 0.60 Å) in a tetrahedral coordination. To explain this result, it is necessary to compare a difference in the interlayer space. The coordination environment around the Co, Cu, and Zn atoms is shown in Figure 6. Two kinds of O−M−O bond angles are remarkably different from the 109.5° angle for a perfect tetrahedron; the tetrahedra are strongly flattened along the *c*-axis. Such a flattening is most likely due to 50% occupancy of the edge-shared tetrahedra in the interlayer space. The strongest flat-

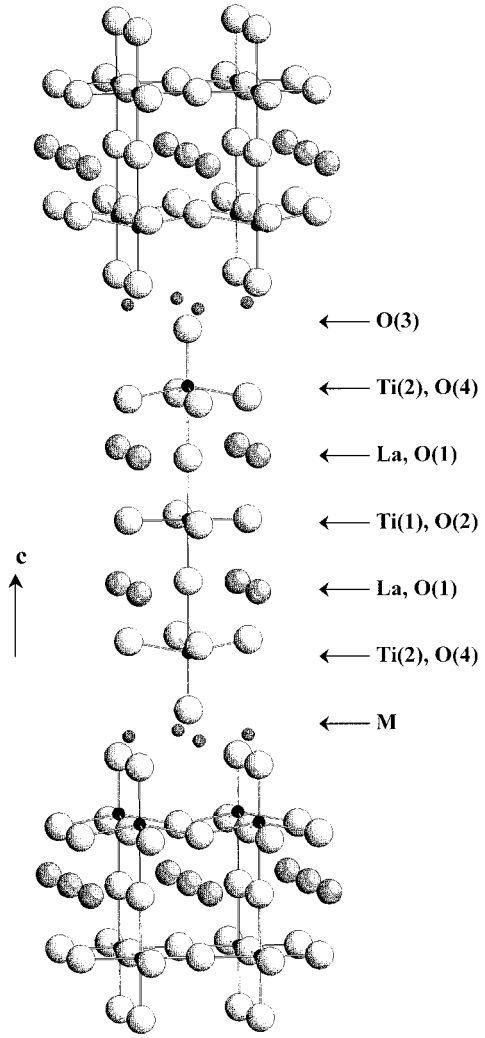

Figure 4. Idealized structure of $MLa_2Ti_3O_{10}$ where M = Co, Cu, and Zn. Only Ti−O bonds are described by lines. (M = small shaded spheres, La = large shaded spheres, Ti = small black spheres, and O = large white spheres).

(19) Shanon, R. D. *Acta Crystallogr.* **1976**, *A32*, 751.

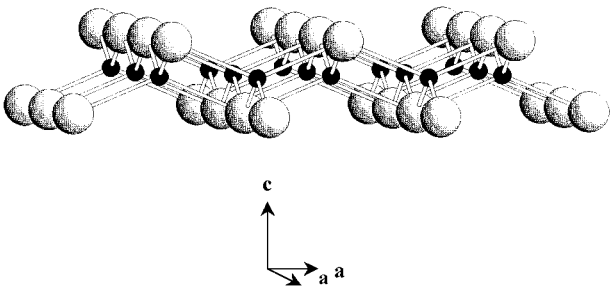

Figure 5. Schematic view of a MO_4 tetrahedra linkage within the interlayer of $MLa_2Ti_3O_{10}$. Only 50% of the tetrahedral sites are statistically occupied by the M atoms. Small and large spheres represent M and O, respectively.

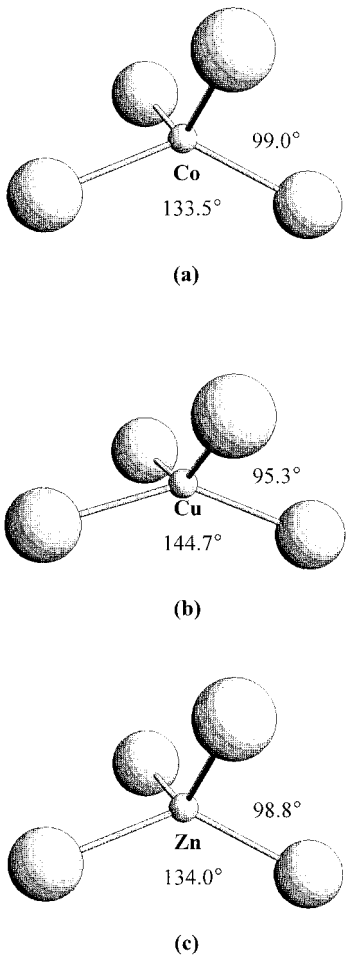

Figure 6. Tetrahedral coordination surrounding the M atom of $MLa_2Ti_3O_{10}$. (a) CoO_4, (b) CuO_4, and (c) ZnO_4 tetrahedron. Small and large spheres represent M and O, respectively.

tening is observed for a CuO_4 tetrahedron. If we consider the interlayer distance (~2.27 Å)[15] of the parent $Na_2La_2Ti_3O_{10}$, $MLa_2Ti_3O_{10}$ represents a collapse of the interlayer space by ~0.63, ~1.05, and ~0.65 Å for M = Co, Cu, and Zn, respectively. Since the *c*-axis doubling gives two transition-metal layers in a unit cell, a contribution of this contraction to a shortening of the *c*-axis would be ~1.26, ~2.1, and ~1.3 Å, respectively. These values are close to a decrease (Δc ~ 1.1, ~2.3, and ~1.1 Å for M = Co, Cu, and Zn, respectively) of the *c* parameters induced by the ion-exchange reaction (Table 1). Hence, it is inferred that the contraction of the unit cell along the *c*-axis is mainly determined by a flattening of the interlayer MO_4 tetrahedra, the thickness of the $[La_2Ti_3O_{10}]$ block not being greatly variable.

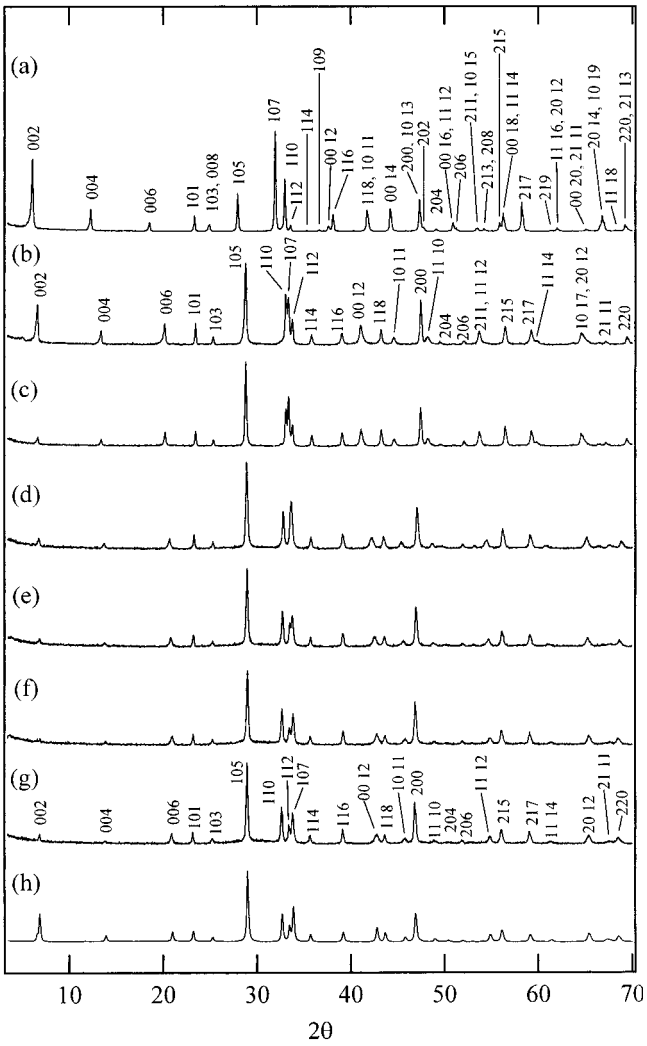

Figure 7. Comparison of the powder X-ray diffraction patterns of (a) parent $Na_2La_2Ti_3O_{10}$ and (b−h) $CuLa_2Ti_3O_{10}$: (b) as-synthesized form, annealed form at (c) 500 °C, (d) 550 °C, (e) 600 °C, (f) 650 °C, and (g) 700 °C for 5 h under an Ar atmosphere, and (h) the simulated form (a = 3.874 Å, c = 25.41 Å, and the interlayer spacing = 0.76 Å).

Thermal Behavior. Differential thermal analyses (DTA) of the as-synthesized forms showed broad weak exothermic curves without an accompanying weight change at around 500−550, 550−650, and 650−700 °C for the Co, Cu, and Zn oxides, respectively. Such a thermal behavior was attributed to an irreversible variation in the cell; a change along the *a*-axis as well as along the *c*-axis was observed when the as-prepared $MLa_2Ti_3O_{10}$ was heated at 600−700 °C under an Ar atmosphere. In particular, the most dramatic variation was seen in the Cu analogue. The temperature-dependent XRD patterns of the Cu phase are compared with that of the parent $Na_2La_2Ti_3O_{10}$ in Figure 7. Owing to the poor crystallinity at a high temperature, a structure refinement was unsuccessful. However, the presence of low-angle reflections suggested that the layer-type structure is retained even after being heated up to 700 °C. The reflection condition found for these phases was $h + k + l = 2n$ for hkl reflections, indicating that the *I*-type unit cell is also retained. Compared with the XRD pattern of the as-prepared phase, furthermore, no other

additional or disappeared reflections are observed with an increasing temperature. Therefore, the same structure model as that of the as-synthesized phase could be supposed for high-temperature ones. In Figure 7, a systematic shift toward a higher angle is found for (00*l*) reflections while (110) and (200) reflectins shift toward lower angles with an increasing temperature. As a result of such shifts, new cell parameters, $a = 3.874(6)$ Å and $c = 25.41(2)$ Å, were obtained after heating took place at 700 °C for 5 h under an Ar atmosphere. These lattice parameters represent an expansion along the *a*-axis by ~0.05 Å and a contraction along the *c*-axis by ~0.91 Å with respect to the as-synthesized form. Assuming that the observed additional shortening of the *c*-axis results from a collapse of the interlayer space, a rough estimate would give ~0.76 Å for the interlayer separation of the high-temperature phase. Thus, if we suppose that the positional parameter of O(3) is (0, 0, 0.235) rather than (0, 0, 0.2269) in Table 2, a simulated X-ray diffraction pattern based on the same (*I*4/*mmm*) space group is given as Figure 7h. Although a difference in (00*l*) reflection intensities is seen, which may indicate a loss of layered character at a high temperature, the simulated pattern is quite similar to the experimental one (Figure 7g). Consequently, it could be concluded that the structural type is retained after annealing at 700 °C. Compared with that (~1.22 Å) of the as-prepared phase, the interlayer spacing of ~0.76 Å is most likely attributed to an increased flattening of CuO_4 tetrahedra to a quasi-square coordination at a high temperature. Copper(II) forms oxometallate ions of various structural types, but mainly containing linked CuO_4 planar units.[20,21] Crystalline CuO provides the simplest example of Cu^{II} forming four coplanar bonds where the O-Cu-O angles are two of 84.5° and two of 95.5°. The copper atom has four neighboring oxygens at 1.96 Å and two next nearest neighbors at ~2.78 Å in its structure. There are also apparently a square planar coordination of Cu^{II} in $CaCu_2O_3$, Sr_2CuO_3, Ba_2CuO_3, and $BaCuO_2$.[22,23] In contrast to Cu^{II}, a common four-coordination of Co^{II} and Zn^{II} in oxides is a distorted tetrahedron rather than a square plane. Some planar complexes for these cations are formed with several chelating ligands.[20] Unfortunately, a complete square planar coordination of Cu^{II} in $CuLa_2Ti_3O_{10}$ could not be demonstrated because of the structural decomposition at a temperature higher than 750 °C.

The structural-type of layered perovskites is generally determined by large ions. Therefore, the proposed structure is quite unusual because the layered structure is retained even after replacing large cations by much smaller ones and heating at a relatively high temperature. The existence of two-dimensional transition-metal oxygen layers, which are completely separated by insulating and nonmagnetic [$La_2Ti_3O_{10}$] blocks, exposes these compounds to further research for electrical, magnetic, and spectroscopic properties in low-dimensional lattices. A large amount of vacancies in the interlayer spaces also opens this structure to further interlayer chemistry. The title compounds should serve as a matrix for such fields of research.

Acknowledgment. This work was supported by the KRISS and the Basic Science Research Institute Program, Ministry of Education (BSRI-98-3421).

CM980581F

(20) Cotton, F. A.; Wilkinson, G. *Advanced Inorganic Chemistry*, 4th ed.; John Wiley and Sons: New York, 1980.

(21) Wells, A. F. *Structural Inorganic Chemistry*, 5th ed.; Oxford University Press: New York, 1984.

(22) Müller-Buschbaum, H. *Angew. Chem., Int. Ed. Eng.* **1977**, *16*, 674.

(23) Müller-Buschbaum, H. Z. *Anorg. Allg. Chem.* **1977**, *428*, 120.